Journal of Innovative Optical Health Sciences
Vol. 4, No. 4 (2011) 337–359

DOI: 10.1142/S1793545811001654

MITOCHONDRIAL FUNCTION AND TISSUE VIABILITY *IN VIVO*: FROM ANIMAL EXPERIMENTS TO CLINICAL APPLICATIONS. FORTY YEARS OF FRUITFUL COLLABORATION WITH BRITTON CHANCE

AVRAHAM MAYEVSKY
The Mina and Everard Goodman Faculty of Life-Sciences
The Leslie and Susan Gonda Multidisciplinary Brain Research Center
Bar-Ilan University, Ramat-Gan, 52900, Israel
mayevskya@gmail.com
mayevsa@mail.biu.ac.il

Accepted 29 May 2011

The involvement of mitochondrial dysfunction in many pathophysiological conditions and human diseases is well documented. In order to evaluate mitochondrial function *in vitro*, many experimental systems have been developed. Nevertheless the number of *in vivo* monitoring systems for the evaluation of mitochondrial activities in intact animals and patients is relatively limited. The pioneering development of the conceptual and technological aspects of mitochondrial monitoring, *in vitro* and *in vivo*, was done by the late Prof. Britton Chance (July 24, 1913–November 16, 2010) since the early 1950s. It was my privilege to join his laboratory in 1972 and collaborate with him for almost four decades. The main achievements of our collaboration are presented in this paper. Our activities included cycles of technology development, followed by its applications to study various pathophysiological conditions. In the initial stage, the first fiber-optic–based NADH fluorometer was developed. This device enabled us to monitor various organs in anesthetized animals as well as the brain of nonanesthetized small animals. Later on, the addition of various physiological parameters to NADH monitoring enabled us to correlate mitochondrial function with other cellular functions. The application of the developed technology to clinical situations was a major interest of Prof. Chance and indeed this goal was achieved in the last decade. As of today, the basic tool for NADH monitoring and the large database of results are available for large-scale experimental and clinical applications.

Keywords: NADH fluorescence *in vivo*; multiparametric brain monitoring; mitochondrial redox state; mitochondrial dysfunction; tissue energy metabolism.

1. Introduction

My first meeting with Prof. Britton Chance was in Israel during his attendance of the Biophysical Society meeting in 1971. He came to visit my Ph.D. advisor, Prof. David Samuel at the Isotope Department of the Weizmann Institute of Science. He saw the brain *in vivo* monitoring system for the evaluation of radioactive phosphate and immediately offered me to come to the Johnson Research Foundation in Philadelphia and join his group as a postdoctoral fellow. After my graduation in October 1972, I and my family (my wife and three children)

came to Philadelphia and stayed there for two years. We arrived in Philadelphia after an 18-hour flight and the Chance family hosted us in their home for more than a week. Their cordial welcome was very important for the establishment of my collaboration with Prof. Chance for more than 35 years. After two years of postdoctoral research, I returned to Bar Ilan University in Israel, but our collaboration continued and the next year-long visit was in 1980−1981. Every year, between 1974 and 1988, I visited the Johnson Research Foundation for an average of one month. Later on, we spent two years in Philadelphia during which time our first attempts to monitor neurosurgical patients came through. During our long collaboration period, Prof. Chance always insisted that we should apply the developed technology to clinical conditions. During my collaboration with Prof. Chance we published 33 papers together, in addition to more than 100 papers that I published with other collaborators on NADH monitoring. I met Prof. Chance in many scientific meetings and a few pictures are shown in Fig. 1. Our meeting in 2007−2008 in China was a kind of a closure of a life cycle that began in Philadelphia in 1972 and ended in the famous Britton Chance Center for Biomedical Photonics, Wuhan National Laboratory for Optoelectronics, Huazhong University of Science and Technology, Wuhan, China.

The aim of this article is to review the scientific and technological papers that I published together with Prof. Britton Chance during our long cooperation.

Fig. 1. My meetings with Prof. Britton Chance between 1972 and 2008. (a) In his office at the Johnson Research Foundation, University of Pennsylvania. (b) During a scientific meeting. (c) During SPIE meeting in San Jose, California, in 2005. (d) In front of the Britton Chance Center for Biophotonics, Wuhan, China, in 2008.

The subjects that we investigated are listed below and a few of them will be presented in detail.

(1) Development of fiber-optic–based fluorometry and its use under pathophysiological conditions of the brain.[1–6]
(2) Monitoring the heart *in vivo*.[7–9]
(3) Two-dimensional monitoring of the brain.[10–16]
(4) Multisite measurements of NADH in the brain.[17,18]
(5) Multiparametric monitoring including NADH.[19–22]
(6) Monitoring NADH inside a nuclear magnetic resonance (NMR) magnet.[23–27]
(7) Clinical monitoring and other subjects.[28–33]

1.1. *Monitoring of mitochondrial NADH*

Table 1 shows the main milestones in the development of the ability to monitor mitochondrial NADH redox state *in vitro* and *in vivo*. It is possible to divide the 100 years of mitochondria research (with reference to energy metabolism) into three periods. In the period from 1906 to 1955, NADH was discovered and its measurement started. In the second period, from 1956 to 1973, a transition was made from monitoring NADH *in vitro* to *in vivo* monitoring in various animal models and various organs. During the third period, from 1974 to the present, the NADH monitoring expanded in various applications, adding new parameters monitored together with NADH. Also during this period, the focus shifted from animal models to monitoring patients, including the clearance of NADH monitoring devices by the FDA.

The crucial development, enabling the monitoring of NADH by many investigators, was published by Chance and Williams in 1955 [Fig. 2(a)]. Under *in vitro* conditions, Chance and Williams defined the metabolic state of isolated mitochondria by

Table 1. Historical milestones in NADH monitoring.

Year	Discovery/Activity	Author(s)
1906	Involvement of adenine containing nucleotide in fermentation by yeast	Harden and Young[48]
1935	Description of full structure of "hydrogen transferring coenzyme in erythrocyte"	Warburg *et al.*[49]
1936	Naming the two cofactors DPN and TPN	Warburg and Christian[50]
1951	A shift in the absorption spectrum of DPNH with alcohol dehydrogenase	Theorell and Bonnichsen[51]
1951	Development of a rapid and sensitive spectrophotometer	Chance and Legallias[52]
1952	Monitoring of pyridinenucleotide enzymes	Chance[53]
1954	The development of double beam spectrophotometer	Chance[54]
1955	The definition and characterization of five mitochondrial metabolic states under *in vitro* conditions	Chance and Williams[55]
1957	The first detailed study on NADH using fluorescence spectrophotometry	Duysens and Amesz[56]
1958	Measurement of NADH fluorescence in isolated mitochondria	Chance and Baltscheffsky[57]
1959	Measurements of muscle NADH fluorescence *in vitro*	Chance and Jöbsis[58]
1962	*In vivo* monitoring of NADH fluorescence from the brain and kidney	Chance *et al.*[59]
1965	Comparison between NADH fluorescence *in vivo* and enzymatic analysis of tissue NADH	Chance *et al.*[60]
1968	Monitoring tissue reflectance in addition to NADH fluorescence	Jöbsis and Stansby[37]
1971	The first attempt to monitor the human brain during a neurosurgical procedure	Jöbsis *et al.*[61,62]
1973	The first fiber-optic−based fluorometer-reflectometer used in the brain of an awake animal	Chance *et al.*[2]; Mayevsky and Chance[1]
1978	2D monitoring of mitochondrial NADH and Fp	Chance *et al.* 1978[11]
1982	Simultaneous monitoring of NADH *in vivo* in four different organs in the body	Mayevsky and Chance[17]
1985	Monitoring of brain NADH together with ^{31}P NMR spectroscopy	Mayevsky *et al.*[23]
1991	Simultaneous real-time monitoring of NADH, CBF, ECoG, and extracellular ions in experimental animals and in the neurosurgical operating room	Mayevsky *et al.*[28]
1996	The multiparametric response (including NADH) to cortical spreading depression is for the first time measured in a comatose patient	Mayevsky *et al.*[63]
2002	Development of the FDA-approved "Tissue Spectroscope" medical device for real-time monitoring of NADH and tissue blood flow	Mayevsky *et al.*[64]
2006	Monitoring of tissue vitality (NADH, TBF and HbO_2) by a new "CritiView" device	Mayevsky *et al.*[47]

Metabolic States of Mitochondria and Associated Oxidation-Reduction Levels of Respiratory Enzymes

Characteristics						Steady state percentage reduction of components				
State	$[O_2]$	ADP level	Substrate level	Respiration rate	Rate-limiting substance	a	c	b	Flavo-protein[a]	$NADH_1$
1	>0	Low	Low	Slow	ADP	0	7	17	21	~90
2	>0	High	~0	Slow	Substrate	0	0	0	0	0
3	>0	High	High	Fast	Respiratory chain	4	6	16	20	53
4	>0	Low	High	Slow	ADP	0	14	35	40	99
5	0	High	High	0	Oxygen	~100	~100	~100	~100	~100

[a]These values are based on the amount of flavoprotein of the respiratory chain. Other fractions, reduced by anoxia, are present but disregarded here.
Source: After Chance and Williams [13].

(a)

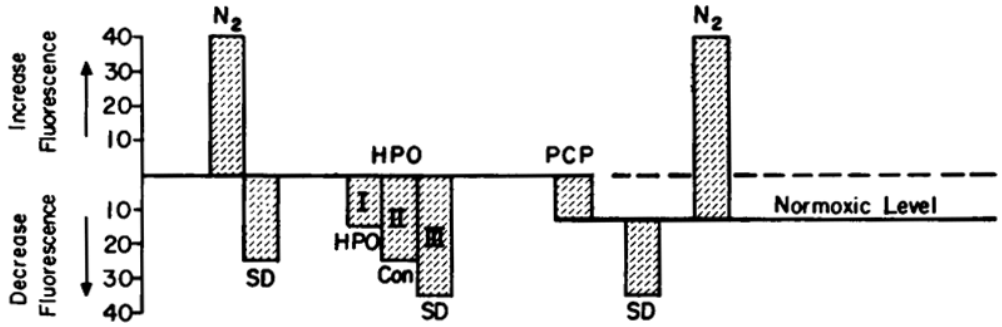

(b)

Fig. 2. The definition of mitochondrial metabolic states in 1955 by Chance and Williams (a) opened a new era in spectroscopic measurements of respiratory chain enzymes' redox states *in vitro* as well as *in vivo*. (b) The effects of various treatments on the oxidation−reduction state of NADH in the brain of a rat. N_2, nitrogen; SD, Spreading Depression; Con, convulsions.

changing ADP, substrate and oxygen levels and measuring the redox state of NADH, flavoproteins and cytochromes. As shown in Fig. 2(a), NAD is converted to the reduced form NADH to reach 99% in the resting state 4. When ADP is added to the oxygenated mitochondrial suspension, NADH is oxidized to a level of 53%, which was defined as the active state 3. The addition of ADP (to mitochondria in state 4) led to an increase in the activity of the respiratory chain in order to synthesize more ATP and resulted in increased oxygen consumption. When O_2 is depleted from the mitochondrial suspension (state 5), NADH increased to the maximal level of 100%. In state 2, the mitochondria have an approximately zero level of substrate, leading to the 100% oxidized state of NADH. Under this state, ADP is available but the limiting factor is the substrate. It is important to note that the metabolic states of the mitochondria *in vivo* are different in their levels of reduced NADH. This issue was discussed by our group[34] and a short summary is given here. The determination of the metabolic state of a tissue *in vivo* requires the ability to change various factors, as has been done in isolated mitochondria. In the *in vivo* experiments, the brain of the awake rat was exposed to various conditions, causing an oxidation or reduction of NADH. The purpose of our investigation was to establish the range between the maximum increase and the maximum decrease in NADH, as compared to the normoxic level. Our previous paper[35] described the responses of the brain to an uncoupler injected into the lateral ventricle after injection of pentachlorophenol (PCP). In order to be certain that the decrease in NADH was in fact due to PCP, the animal was exposed to a N_2 cycle every few minutes. After each N_2 cycle, which causes a large increase in fluorescence, the oxidation cycle was recorded. The results show that PCP injection increases the range between maximal and minimal levels of NADH.

Before PCP injection, the range was 55−60%, while after the injection it was 72−74%.

Figure 2(b) summarizes the effects of the NADH oxidation−reduction state under various treatments given to a nonanesthetized rat. Breathing Nitrogen led to a 40% increase in NADH, whereas spreading depression (SD) was accompanied by a 25% decrease. Under hyperbaric oxygenation (HPO) conditions, three levels of NADH oxidation were recorded. During Phase I, the preconvulsive period, a 15% decrease in NADH was recorded. The convulsions (Phase II) led to another 10% decrease, and during the third phase (probably SD) the total oxidation of NADH was 35% as compared to the normoxic level. The uncoupler led to a 10% oxidation of NADH. Therefore, under our experimental conditions, the maximal increase of NADH in the brain was 40%, while the maximal decrease was about 35%.

2. Technological Development and Typical Results

The effect of blood on NADH fluorescence was discussed in our review.[34] In order to monitor NADH *in vivo*, Chance's group had to avoid areas containing large blood vessels that interfere with the emission and excitation light. The monitoring of a second channel in tissue fluorometry *in vivo* was reported by Chance *et al.* in 1963.[36] They showed that "changes due to the deoxygenation of oxyhemoglobin do not interfere with measurement of the time course of fluorescence changes in the tissue studies". The addition of a second monitoring signal, namely tissue reflectance at the excitation wavelength, was reported in 1968 by Jöbsis and Stansby,[37] who also collaborated with Prof. Chance.

After the development of the *in vivo* monitoring system of NADH, Chance's vision was to monitor the brain in nonanesthetized animal. According to his specifications, Schott Jena Glass in Germany constructed the first fiber-optic probe transmitting ultraviolet (UV) light. This was achieved in 1972, when UV transmitting quartz fibers became available (Schott Jena Glass, Germany). We have used the light-guide-based fluorometer for *in vivo* monitoring of various organs using different optical systems. The original device designed by Chance, functioned on the time-sharing principle [Fig. 3(a)]. The second and third options were called the DC fluorometer/reflectometers, presented in Figs. 8(a) and 9(a) respectively.

2.1. *The time-sharing fluorometer/ reflectometer*

This type of fluorometer, shown in Fig. 3(a), was designed and tested in October 1972 using the rat brain. The details were described by Chance *et al.* in

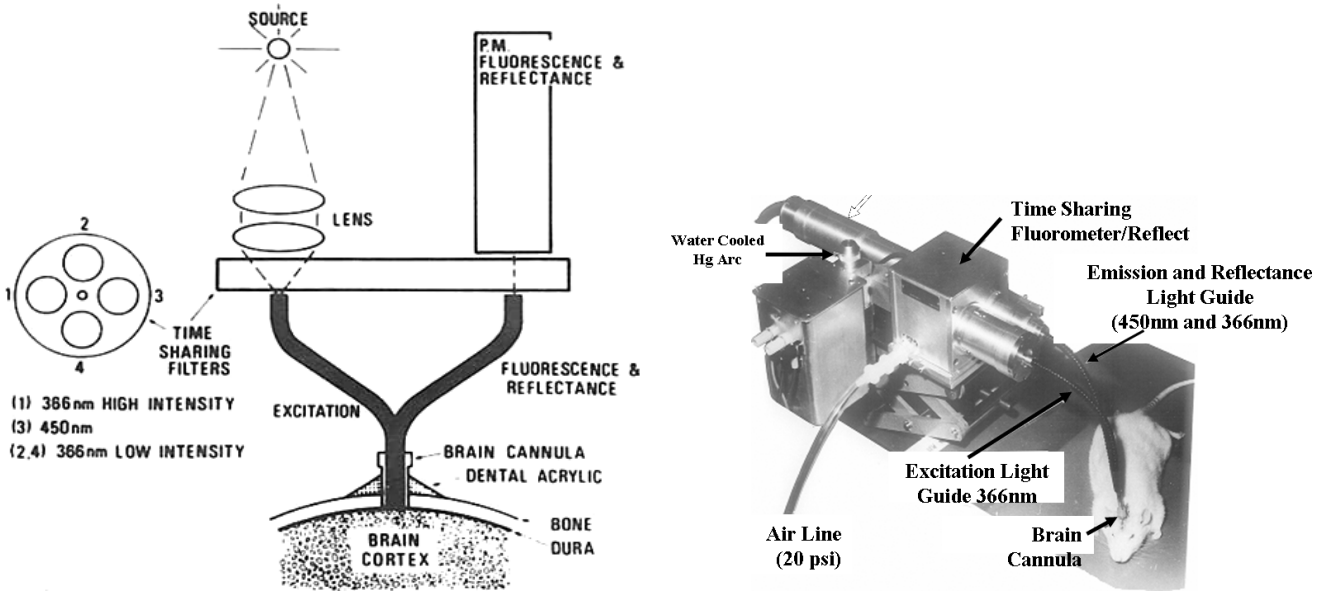

(a) (b)

Fig. 3. In (a), the scheme of the original time-sharing fluorometer/reflectometer is presented {Chance, 1973 1061/id}. In (b), an operated rat implanted with a cannula connected to the time-sharing fluorometer/reflectometer developed in 1972 is presented.[6]

1973.[2] In this model, four filters were placed in front of a two-arms light guide. Filters 1 and 3 enabled the measurement of NADH fluorescence, while filters 2 and 4 were used to measure tissue reflectance at the excitation wavelength. The reflectance trace was used to correct the NADH signal for hemodynamic artifacts and to indicate changes in the blood volume of the sampled tissue. In this original system, only one photomultiplier tube was used for the detection of the two signals. Figure 3(b) presents one of the first *in vivo* brain monitoring time-sharing setups, connected to the brain of an anesthetized rat.[6] In order to simplify the monitoring system, the time-sharing approach (AC mode) was replaced by splitting the light emitted from the tissue into two unequal fractions for the measurement of fluorescence and reflectance signals. This model, named the DC-type fluorometer, had a three-way light guide [Fig. 8(a)], which was later replaced by a two-arms light-guide probe [Fig. 9(a)]. In all the three configurations, the reflectance signal was used for the correction of the fluorescence signal.

2.1.1. *The effects of anoxia and cortical spreading depression*

In Fig. 4, the effects of anoxia and cortical SD are shown. The rats were slightly anesthetized by Equithesin. Nitrogen was applied via a nasal mask. Figure 4(a) shows the effect of N_2 on the NADH fluorescence, reflectance, electroencephalogram (EEG) and blood pressure.[38] The top trace shows the reflectance, decreasing in all animals during the N_2 cycle. This decrease of reflectance proceeded in two phases. The first decrease was small (in comparison to the second) and occurred while the animal was breathing spontaneously. A second decrease occurred after the animal stopped breathing (SB). The recovery of the reflectance to the baseline occurred about 10 min after the rat started breathing again. The second trace from the top, the fluorescence, shows a large increase in NADH fluorescence during the first phase of the N_2 cycle. In order to correct for hemodynamic artifacts induced by anoxia we used a correction technique.[34] The reflectance signal at 366 nm was subtracted from the fluorescence signal at 450 nm at a 1:1 ratio. The difference between the fluorescence and reflectance signals is shown in the third trace, the "corrected" fluorescence. After the cessation of respiration, a large decrease in reflectance occurs; an apparent decrease in fluorescence (oxidation) is observed, which is almost undetectable in the corrected trace. The small decrease shown in the corrected trace is due to the imperfection of the correction factor in this particular animal. After the N_2 administration had been discontinued (SN), artificial respiration (AR) was applied to induce spontaneous breathing. After the animal started breathing, a quick decrease in NADH level is observed in the uncorrected as well as in the corrected fluorescence. The recovery of the NADH level to the baseline is very fast in comparison to the recovery of the reflectance. The EEG of both hemispheres reaches a very low amplitude when the NADH level reaches 80−90% of the maximum increase during the N_2 cycle. The EEG responses of the two hemispheres were identical. The recovery of the EEG follows the NADH recovery to the normoxic level.

The application of 0.3 M KCl produces three separate waves of SD [Fig. 4(b)], which were stopped by NaCl washing.[39] In these three cycles, the initial phase of each response is obscured by the reflectance change (the second trace from top). Through the subtraction of the reflectance trace at a 1:1 ratio, we obtain in the third trace from the top three symmetrical cycles of NADH oxidation and reduction. Although it is possible that there are geometrical problems with the interpretation of the exact timing of the electrical waves with respect to the optical data, it is of interest to note that the maximal mitochondrial activity occurs near the nodes of the SD waves. These two figures show that each cycle of the SD involves a state 4-3-4 metabolic transition at the mitochondrial level. The extent of the metabolic transient can be evaluated by comparing the fluorescence decreases in an SD cycle with the fluorescence increases in a normoxic−anoxic cycle (40% ± 10%) with respect to the normoxic level. The fluorescence decrease in SD is 20% ± 10%. It is characteristic of the state 4-3 transition in isolated mitochondria. In SD, we observe a 20% decrease as compared with a 40% increase in anoxia. The difference between these values and those expected for a state 4-3 transition is presumably because (1) the brain is not in state 4 but is between states 4 and 3; (2) fixed fluorescence signals from the brain (due to collagen components, etc.) that do not respond metabolically diminish the fractional change observed in SD; (3) state 3 is not reached in SD. The rapid responses of the

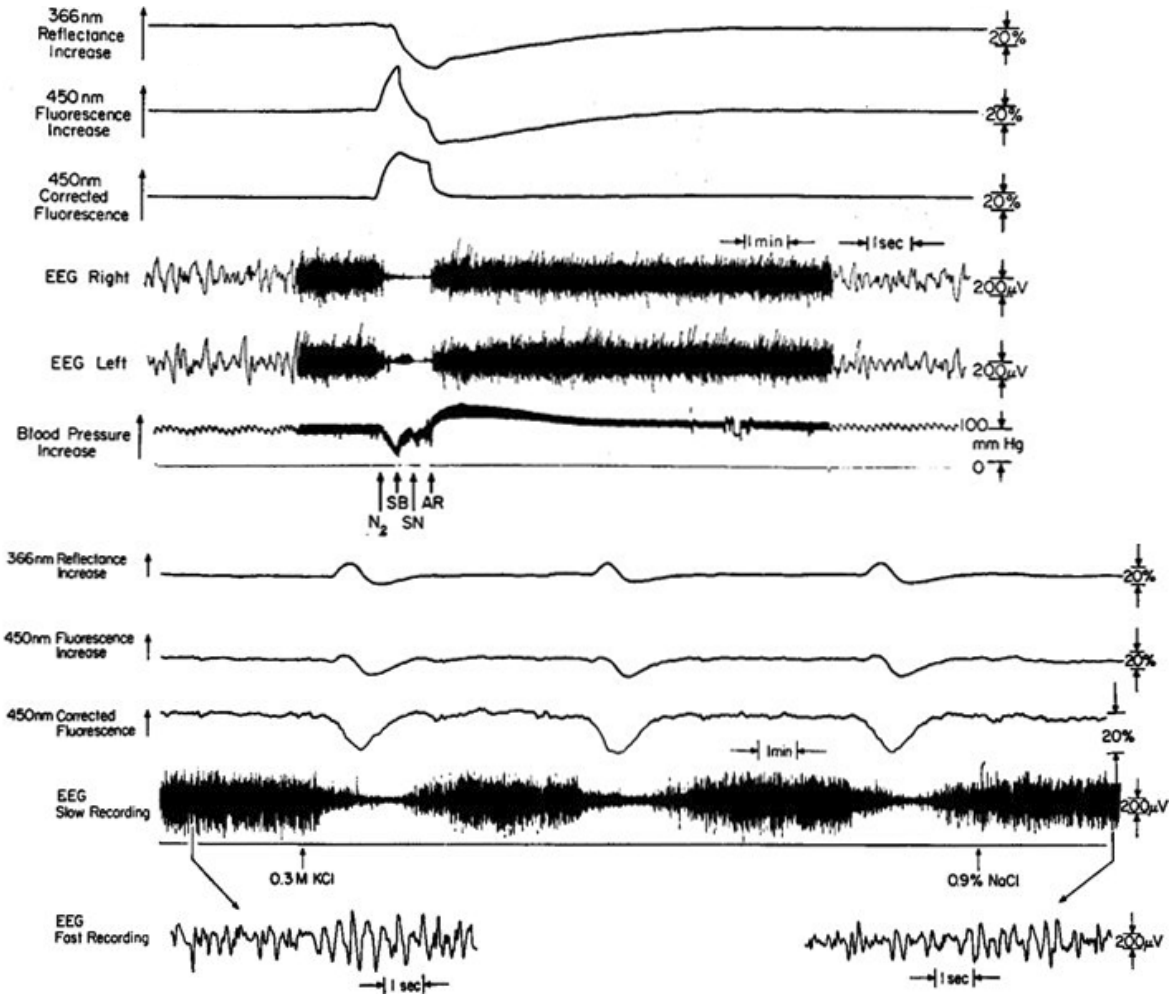

(a)

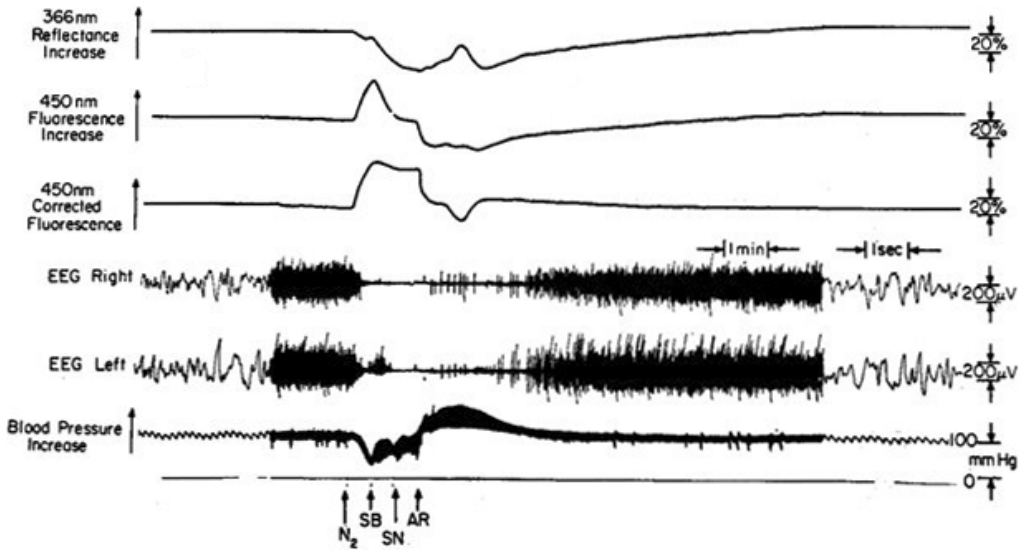

(b)

Fig. 4. The effects of anoxia on NADH fluorescence, 366-nm reflectance, EEG, and blood pressure. In (a), the duration of the anoxia was 70 s and in (c), 100 s. SB, the animal stopped breathing; SN, nitrogen stopped; AR, short artificial respiration.[61] (b) The response of the brain to the application of 0.3 M KCl solution, epidurally. Three cycles of NADH oxidation (cortical SD) were developed. The arrow direction shows an increase in the optical signals. Note that the third trace is on an expanded scale.[62]

fluorescence technique now permit a much better resolution of the metabolic consequences of SD than was possible in earlier studies. Figure 4(c) shows the response of the same animal to a longer N_2 cycle. The animal was exposed to N_2 for 100 s. The main differences between the two cycles [Figs. 4(a) and 4(c)] are that, after the recovery of NADH to the normoxic level, a further decrease in NADH occurred (the third trace) and at this time the EEG was depressed and recovered to normal values only later. This cycle of NADH oxidation following the N_2 cycle was observed in most animals after exposure to a long N_2 cycle. The patterns of changes in reflectance, fluorescence and the corrected traces were similar to those observed in the SD elicited by KCl, as also shown in Fig. 4(b).

In order to study in detail the effects of SD events, two types of electrodes were added to the time-sharing fluorometer. This project was performed in collaboration with Prof. Mela, who was collaborating with Prof. Chance in the University of Pennsylvania. As shown in Fig. 5(a), the monitoring system included electrodes for DC steady potential and extracellular potassium.[19] An SD wave was initiated by passing a solution of 0.5−0.6 M KCl epidurally through the cannula. Figure 5(a) shows a typical response of the brain to 0.6 M KCl. Three SD cycles were developed and then stopped by washing the dura with 0.85% NaCl. The first cycle was recorded 2 min after the application of KCl. The DC potential showed a negative shift followed by a plateau and a slower recovery phase which had a small positive wave. The extracellular potassium concentration increased very quickly and after a plateau phase decreased slowly to the original level. The electrocortical surface electrode (ECoG) showed depression responses and recovered to the normal pattern 10−15 min after washing the dura mater with NaCl. The 366-nm reflectance, NADH fluorescence and the corrected fluorescence show the response of SD as described previously. The corrected fluorescence trace shows a decrease of 25% in NADH in comparison to the normoxic level. This decrease in NADH level, which represents an oxidation (25%) is identical in the three cycles. The first cycle was longer but the level of oxidation was the same.

2.1.2. *The effects of complete ischemia*

Along with Prof. Chance we repeated his experiments on brain ischemia using the awake rat model. Figure 5(b) shows a typical response of the awake brain to complete ischemia induced by decapitation. The upper trace shows that the reflectance of 366-nm light increases immediately after decapitation by 20% and reaches a plateau within 10 s. In most animals this increase was smaller than 20% and in a few it was even undetectable. After 2 min, a secondary increase in reflectance was recorded. This secondary increase was recorded in 10 out of 12 animals. The second trace from the top shows the response of the 450-nm fluorescence. In this animal, the maximum level of fluorescence was 130% above the normoxic level. The third trace shows the corrected fluorescence (the difference between the first and the second traces) response to decapitation. At the same time that the reflectance trace showed the secondary increase, the corrected fluorescence trace showed a transient decrease which returned to its maximum level within a few minutes. The lower two traces show the ECoG response to decapitation. The right hemisphere was the side from which the NADH fluorescence was measured. In most animals, the ECoG traces showed a mechanical artifact when the decapitation was performed. In this animal, the ECoG became flat within 10−15 s and the two hemispheres showed an identical response.

2.1.3. *The effects of epileptic activity*

Prof. Chance's vision was to expand our knowledge on brain pathology in animal models in order to monitor ill patients in the future. The effects of locally applied Metrazol were tested in non-anesthetized animals. Metrazol (100 mg/ml) was applied epidurally using a specially designed cannula. The typical response to Metrazol occurs 3−5 min after the administration of the drug and the results are shown in Fig. 6(a).[5] Metrazol was applied to the right hemisphere and the left one served as a control. After the application of Metrazol, an increase in electrical activity was found, resulting in an oxidation of NADH which was in the range of 5−10% of the normoxic level. After a period of very high activity, the EEG became isoelectric, while the NADH showed a very large oxidation cycle which then recovered to the normoxic level. In some animals, a different response was recorded, as shown in Fig. 6(b). In these cases, a small oxidation under the Metrazol exposure was recorded, but the recovery to the normoxic level showed no

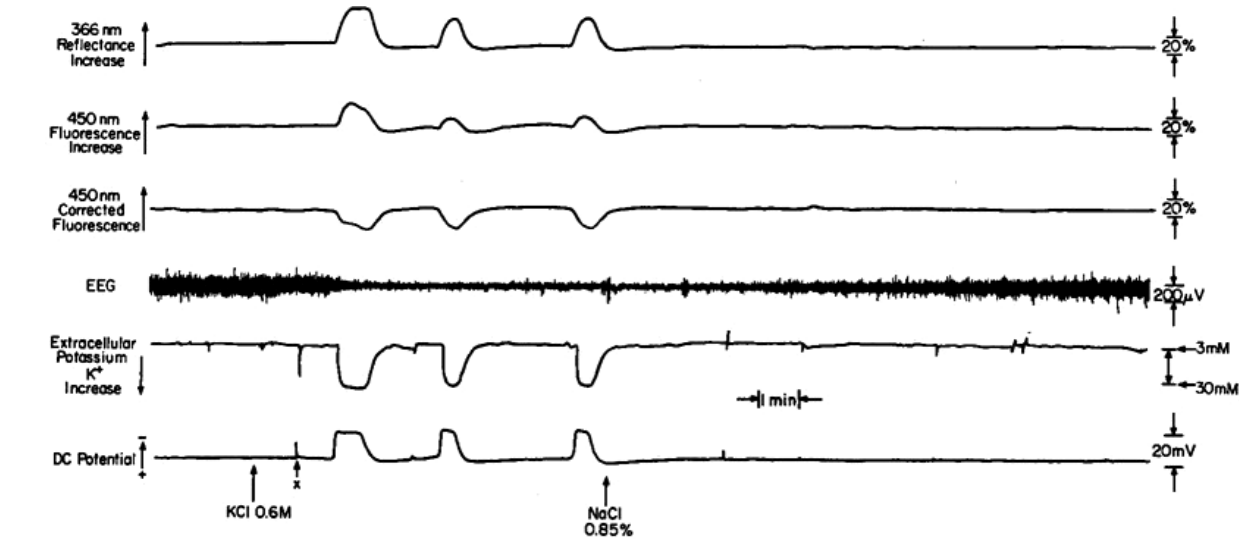

(a)

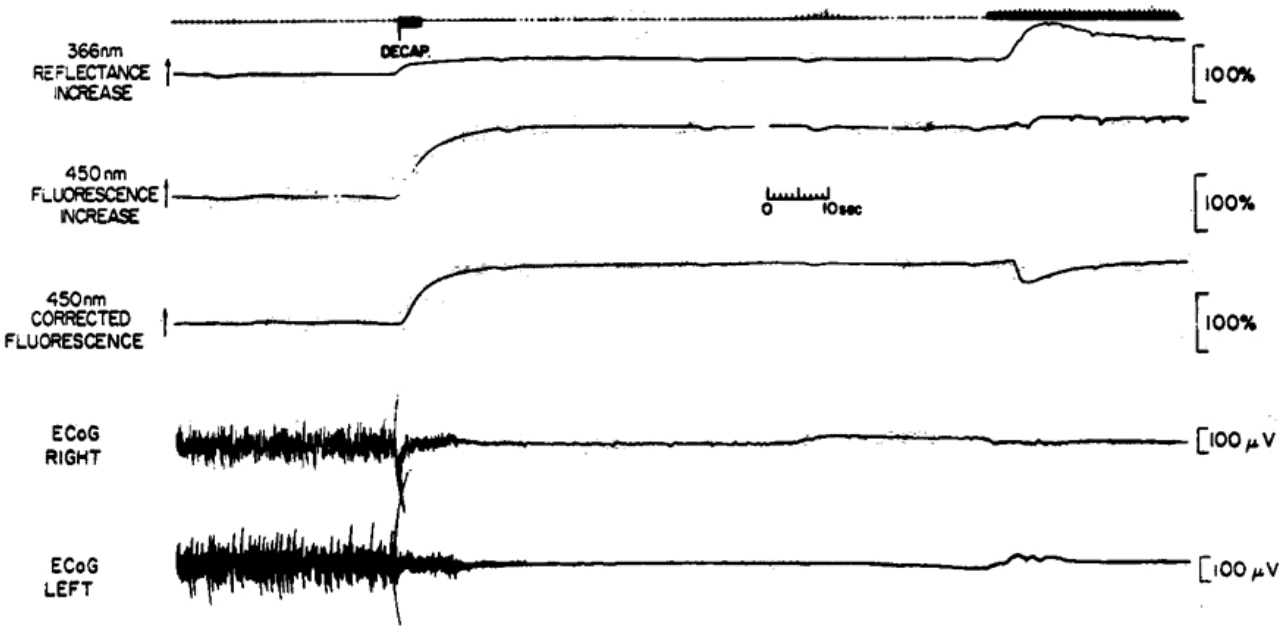

(b)

Fig. 5. (a) The effects of cortical spreading depression (elicited by 0.6 M KCl) on the extracellular potassium, DC potential, ECoG and NADH fluorescence of the exposed rat brain cortex. X, Electrostatic interference from the experimenting observer.[19] (b) The effects of decapitation on the oxidation−reduction state of NADH and ECoG recorded from the cortex of the awake rat.[6]

large oxidation cycle. The reflectance changes were very small during the effect of Metrazol.

2.1.4. *The effects of hyperbaric oxygenation*

The involvement of mitochondria in the oxygen toxicity process was investigated in detail by Chance and Jamieson in the 1960s. We continue this project using the awake rat model that we developed in Philadelphia (see Mayevsky and Rogatsky). The rat was placed in a small hyperbaric chamber (Bethlehem Corp. FM-21-A) and connected to the light pipe. The indwelling cannula receives the bifurcated light pipe which exits through the wall of the chamber onto the time-sharing fluorometer. The general pattern of responses to oxygen toxicity is illustrated in Fig. 7.[3] The upper trace shows the reflectance at 366 nm. In this experiment,

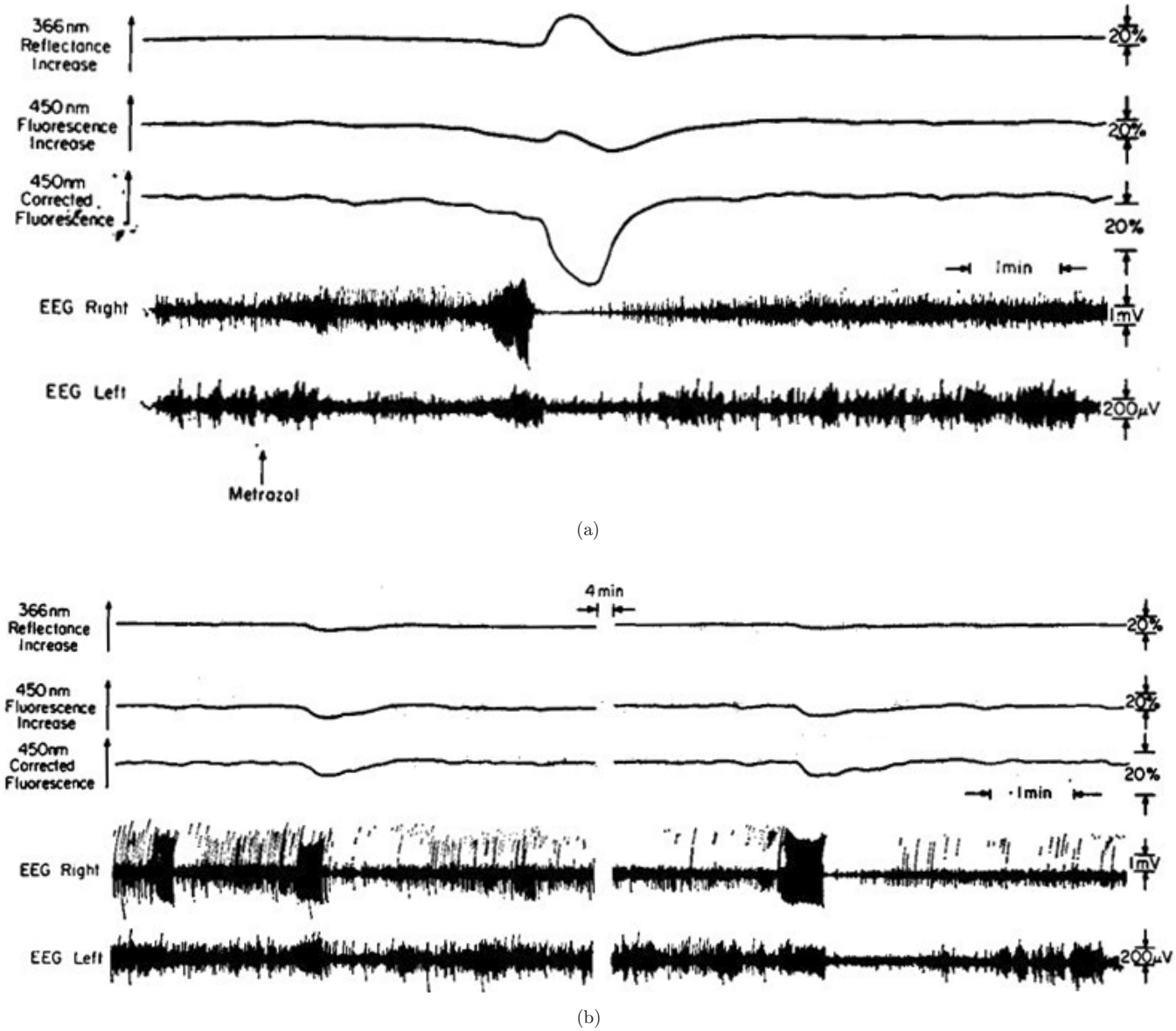

Fig. 6. The effects of Metrazol on the brain NADH fluorescence, 366-nm reflectance and the EEG of the two hemispheres. Note that the amplitude of the EEG calibration in the right hemisphere is 1 mV. The typical response is shown in (a). (b) Another type of response to Metrazol applied 10 min before the recording was made.[5]

very little change was observed during compression but a small increase (8%) occurred 3 min later. This increase corresponds to a change in hemodynamic response in the direction of vasoconstriction and reduced blood flow. Fifteen minutes after compression, a large decrease in reflectance (25%) occurred. In this animal, the reflectance returned to the precompression level after further 18 min and remained at this level until the respiration ceased. However, in the majority of preparations, the postcompression decrease in reflectance, which is probably due to vasodilatation, remained at the lower level throughout the remainder of the experiment. During the compression, a 4−5% decrease of NADH fluorescence was observed. However, as the maximum reflectance change occurred just after this point, the uncorrected fluorescence appeared to return to the baseline. This observation indicates that the 450-nm fluorescence emission is affected by the intensity of the light absorbed by the blood and scattered by the tissue, as monitored by the reflectance measurements. Thus, some of the changes of the NADH redox state are obscured in the uncorrected fluorescence trace. Consequently, the third

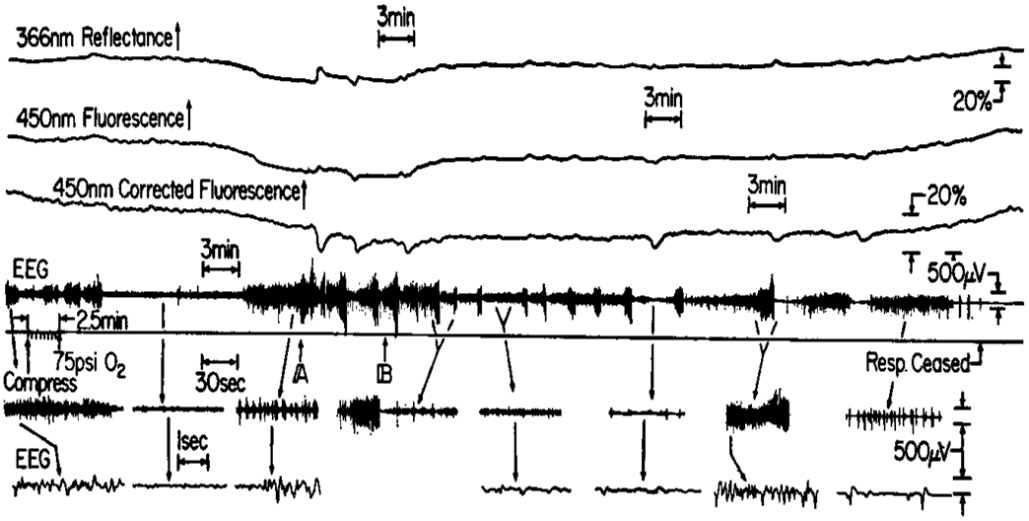

Fig. 7. The response of the cortex of a nonanesthetized rat exposed to hyperbaric oxygen at 6 ATA (75 psi) until cessation of respiration and EEG signal. Reflectance and fluorescence calibrations are indicated as percentages of the normoxic signal. The calibrations for both these traces are identical. The two lower traces are sections from the EEG recording, taken on faster time bases than in trace 4, with a recorder connected in parallel.[3]

trace, showing the corrected fluorescence, gives a more accurate indication of the true oxidation state of pyridine nucleotides. An 8% oxidation of NADH started immediately upon compression and reached a steady level 5 min after the level of 6 ATA (absolute atmosphere) oxygen was reached. After 10 min, a further oxidation occurred, concomitant with the decreased reflectance signal and with the onset of convulsions, as shown in the EEG trace. Six minutes after the onset of the seizures, a series of oxidation−reduction cycles of NADH was observed. Six such cycles were observed during this experiment. At the peak of such an oxidation cycle, the maximum fluorescence decrease was to 30% of the normoxic level. After the cessation of respiration, a slow, continual increase in NADH fluorescence was seen. The fourth trace in Fig. 7 shows the EEG on a very slow time scale. Prior to compression, the EEG was composed of mixed high and low amplitude waves. Within 4 min of reaching 6 ATA oxygen, the EEG changed to a low-amplitude, high-frequency response, indicative of a hyper-alert state. Visual observation of the rat during this period also showed the typical hyperactive behavior of rats exposed to HBO. Sixteen minutes after the compression, the first signs of seizures were noted on the EEG. These early signs consisted of isolated spikes, which gradually increased in intensity and number to give a typical grand malconvulsive pattern. It should be pointed out that the oxidation−reduction cycles of trace 3, mentioned earlier, occurred between the bursts of convulsion. Such NADH cycles continued until the eventual cessation of respiration and EEG occurred. These cycles, which are superimposed on the hyperbaric oxidized level and occur between bursts of convulsive activity, have not been described previously in HBO. These cycles in the redox state of NADH, which are concurrent with changes in reflected light and depression of the EEG, are characteristic of the effects seen after the application of KCl solution to the cortex of nonanesthetized rats and are believed to represent SD. Traces 5 and 6 in Fig. 7 show portions of the EEG recording taken on a faster time base to show details of the frequency and amplitude of the EEG.

2.2. *From the time-sharing to DC fluorometry/reflectometry*

One of the main advantages to work in the Johnson Research Foundation was the availability of the mechanical and electronic workshops located on the same floor. This was the genius approach of Prof. Chance that facilitated the performance of all scientists collaborating with him. In order to simplify the NADH monitoring system, we developed a fluorometer that was not based on rotating excitation and emission filters. The name given to the new device was the "DC fluorometer" in contrast to

the "AC fluorometer" or the time-sharing fluorometer with rotating filters.

2.2.1. *The DC fluorometer Type A*

The diagram in Fig. 8(a) identifies the elements of the fluorometer.[7] The light source is a medium-pressure "short-arc" mercury arc, which illuminates a segment of the branched light guide containing 5% of the fibers through Wratten 18A and Corning 5874 filters which select the 366-nm line of the mercury arc spectrum. The excitation light is coupled by fibers transparent to 366-nm light to the surface of the organ under observation, the heart in the present case. For excitation, 50% of the fibers are randomly distributed among the remaining fibers. The light guide may be maintained against the heart with a gentle pressure in small animals or, in larger animals, it is either sewn to the heart or surrounded with appropriate "tissue glue" to keep it in contact with the heart through the course of heart motions. In large animals, the pericardium is removed, but this is not necessary for the rat heart. The remaining optical fibers receive reflected signals from the excitation wavelength and from the emitted fluorescence. These are conducted from the animal to two further branches, one containing 10% and the other 40% of the fibers. The former illuminates a photomultiplier through a 366-nm filter (Wratten 18A) and the latter illuminates a second photomultiplier through Wratten 2C and 47 filters transmitting light at 450 nm, respectively, for "reflectance" and "uncorrected fluorescence" signals. The output voltages of the two photomultipliers were adjusted so that they both give a 1 V signal to the difference amplifier [Fig. 8(a)], which has a 1:1 gain and gives a zero output signal for equal inputs. The output of the difference amplifier is termed the "corrected fluorescence". Changes in the three parameters are computed as percent of the full-scale reading due to the normoxic fluorescence of the tissue surface. In the case of the compensated trace, the full-scale reading is readily determined by decreasing the dynode voltage on either the reflectance or the uncorrected fluorescence photomultiplier to zero. The response time of this fluorometer covers a much wider range than is feasible for previous fluorometers because of the effective optical coupling afforded by the branched light guide. Response times down to 1 ms are feasible for perfused organs and about 1 s for organs *in situ*.

This apparatus has been applied to a variety of experimental models. The possibility of titrating the intracellular redox state with the percentage of oxygen in the inspired air now enables a non-destructive evaluation of the manifold factors that regulate oxygen delivery to the tissue. Although this example emphasizes the use of the heart surface for measuring oxygen delivery to the tissue, other organs may be used, particularly the surface of the brain where the technique has already been developed for observations in chronic and acute conditions. The response of the animal to a decrease of inspired oxygen is illustrated by the traces shown in Fig. 8(b). Under anoxia, NADH was increased to the maximal level. The uncorrected fluorescence increase is considerably larger and the combined traces — the corrected fluorescence — correspond to an increase of fluorescence of about 80%. It should be noted that the return of the reflectance trace occurs somewhat after there is a return of the uncorrected trace. These irregularities are, however, "smoothed out" in the corrected fluorescence trace. The anoxia is repeated with similar results except

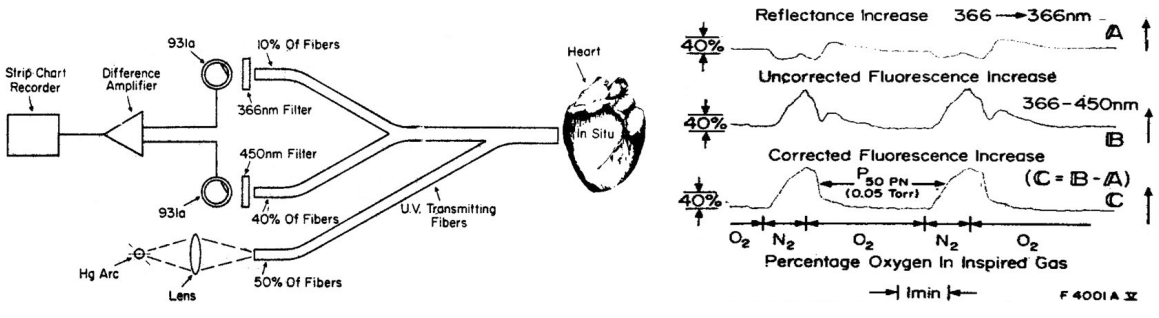

(a) (b)

Fig. 8. (a) A schematic diagram of the optical coupling of the simplified fluorometer to the heart tissue. (Refer text for other details.) (b) The maximal response of the intracellular redox state to nitrogen breathing.[7]

for a somewhat larger overshoot in the reflectance trace. However, the correction leads to identical kinetics in trace C.

2.2.2. *The DC fluorometer Type B*

The principles of the single-channel DC fluorometer Type B are shown schematically in Fig. 9(a).[40] Also, a four-channel fluorometer, shown in Fig. 9(b) was constructed.[41] This unit was quadrupled from the single channel and small variations were introduced in the light guide, as described below. The light source was a 100-W water-cooled or air-cooled mercury arc having a 366-nm filter in front of it, between the fluorometer and the excitation fibers bundle. The light guide contains four bundles of excitation fibers split from the light source. Another four bundles of fibers transmit the emitted light form four Y-shaped light guides. We used quartz fibers having a diameter of 2 mm in each common part, as well as plastic ones having a diameter of 0.8 mm in each common part. The emitted light from the tissue was split in a ratio of 90:10 and was used to measure fluorescence at 450 nm and reflectance at 366 nm, respectively. We corrected for artifacts in the NADH fluorescence measurement by using the 1:1 subtraction technique to obtain the corrected fluorescence trace.

The four-channel fluorometer was used to obtain recordings in five rats and five gerbils. In the rat, we monitored NADH in the brain, liver, kidney and testis simultaneously. In the gerbil, we monitored four points on the same brain hemisphere. The animals were anesthetized and the light guide for monitoring the brain was connected by a holder cemented to the skull with dental acrylic cement. Figure 10 shows the results obtained from a rat ventilated via a respirator after intravenous injection of Flaxedil to stop spontaneous breathing. Figure 10 demonstrates the effects of graded hypoxia and anoxia on the reflectance and corrected fluorescence. The uncorrected fluorescence was measured from each organ but was not recorded on the same chart paper. A typical response to hypoxia, namely an increase in the corrected fluorescence and at the same time a decrease of reflectance, was obtained when the rat was ventilated with 10% oxygen (in nitrogen). The largest change in the corrected fluorescence signal was measured during a complete deprivation of oxygen, achieved by ventilating with 100% nitrogen. The response to 5% oxygen was intermediate. Thus, there appears to be a

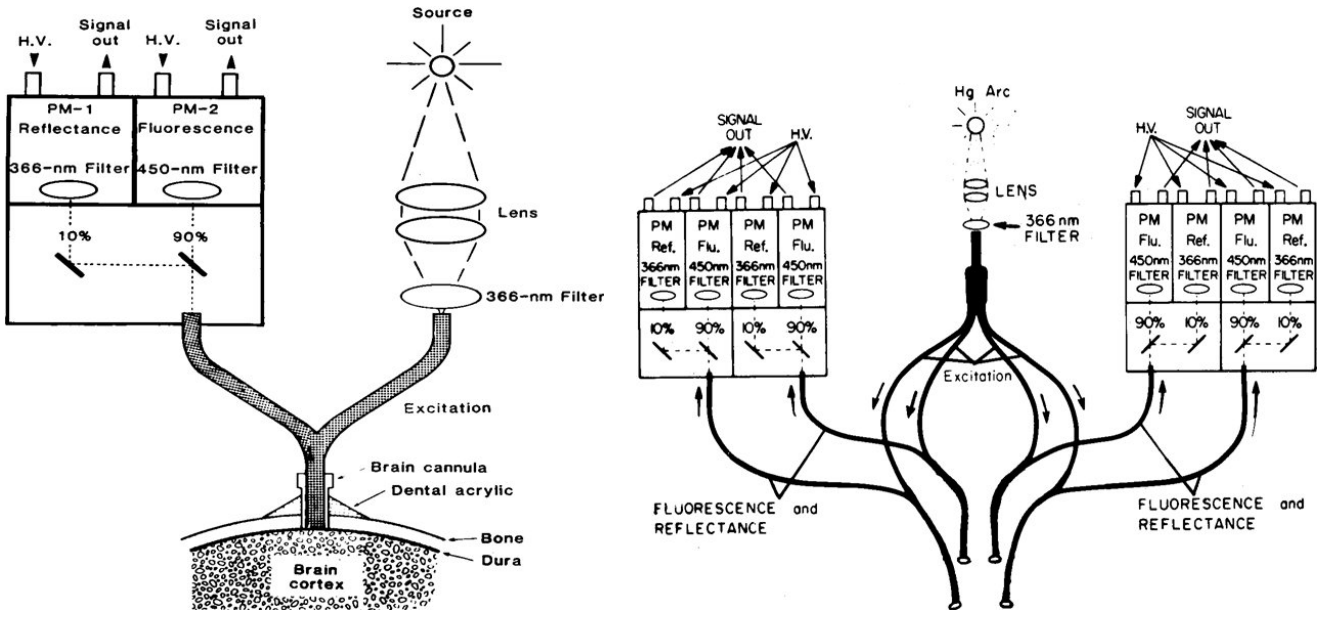

Fig. 9. Schematic representation of the single-channel DC fluorometer-reflectometer (a), which served as the basis for the multichannel instrument used in the present study. HV, high-voltage input; PM-1 and PM-2, photomultipliers.[63] (b) The four-channel DC fluorometer/reflectometer for studying the NADH redox state simultaneously from four different organs or four separate spots in the same organ, such as the brain.[64]

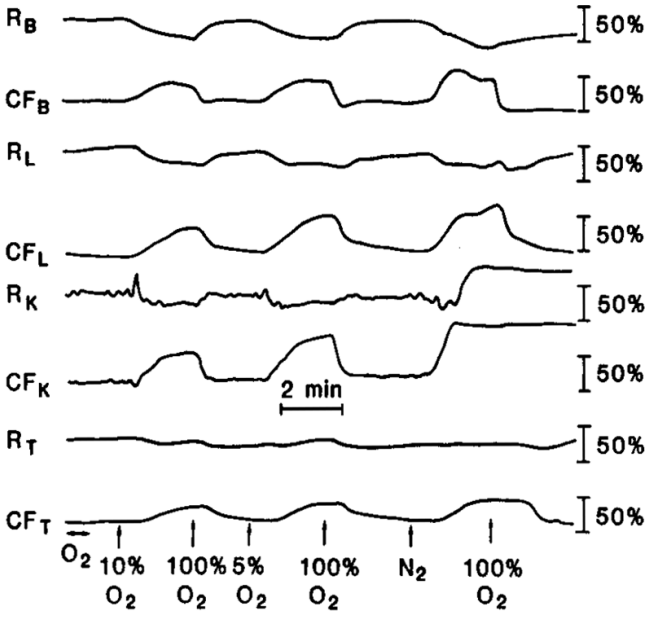

Fig. 10. Effects of graded hypoxia and anoxia on the NADH redox state in an artificially ventilated rat. Four organs were monitored simultaneously, and for each organ we recorded the reflectance (R) and the corrected fluorescence (CF). Subscripts: B, brain; L, liver; K, kidney and T, testis.[17]

direct correlation between the partial pressure of oxygen (pO_2 in the air breathed) and the magnitude of change in the NADH redox state. These typical responses were found in all the four organs tested, with little variation between them. In all of the normal rats tested, the same qualitative response to anoxia was found in the normoxic brain.

The magnitude of the decrease in the reflectance signal was not greatly affected by the level of pO_2, probably because autoregulating vasodilation took place during hypoxia to increase the blood volume to the organ. This vasodilation was activated even by ventilating the animal with 10% oxygen, and a decrease in the reflectance was recorded. In the testis, the reflectance response was minimal and was probably due to the small amount of vascularity in the measurement site (observed during the exposure of the organ). The kidney showed an atypical reflectance response in this animal; that is, when the rat breathed nitrogen only, a large increase in reflectance was recorded simultaneously with the expected large increases in the corrected fluorescence. The recovery of the reflectance to its base line was very slow (not shown); this response was not observed in all kidneys tested. The same animal was exposed to anoxic cycles a few times before this record was taken, and this large change in reflectance was not found earlier. The kidney of this animal did not recover to its normal state (Fig. 10).[17] In the five animals used in this part of the study, the kinetic responses in NADH fluorescence during the transition from the normoxia to anoxia were different in the four organs tested.

2.3. *From single-parameter to multiparametric monitoring systems*

After long discussions, Prof. Chance realized that we must monitor more physiological parameters in order to understand the responses of the brain to pathophysiological conditions. He enabled me to spend one year in the JF supporting the R&D of these systems. In order to improve the multiparametric probe, it was necessary to include the various sensors in a single holder that could be used on a daily basis without too many technical difficulties. In the new probe, all sensors touched the brain surface (after removal of the dura mater without penetration into the tissue itself). Using the same principles, we were able to develop a new generation of multiprobe assemblies that have been used in our laboratory during the past 25 years (Figs. 11 and 12). The next significant step was the embedding of a laser Doppler flowmeter sensor into the multiprobe assembly to monitor the continuous

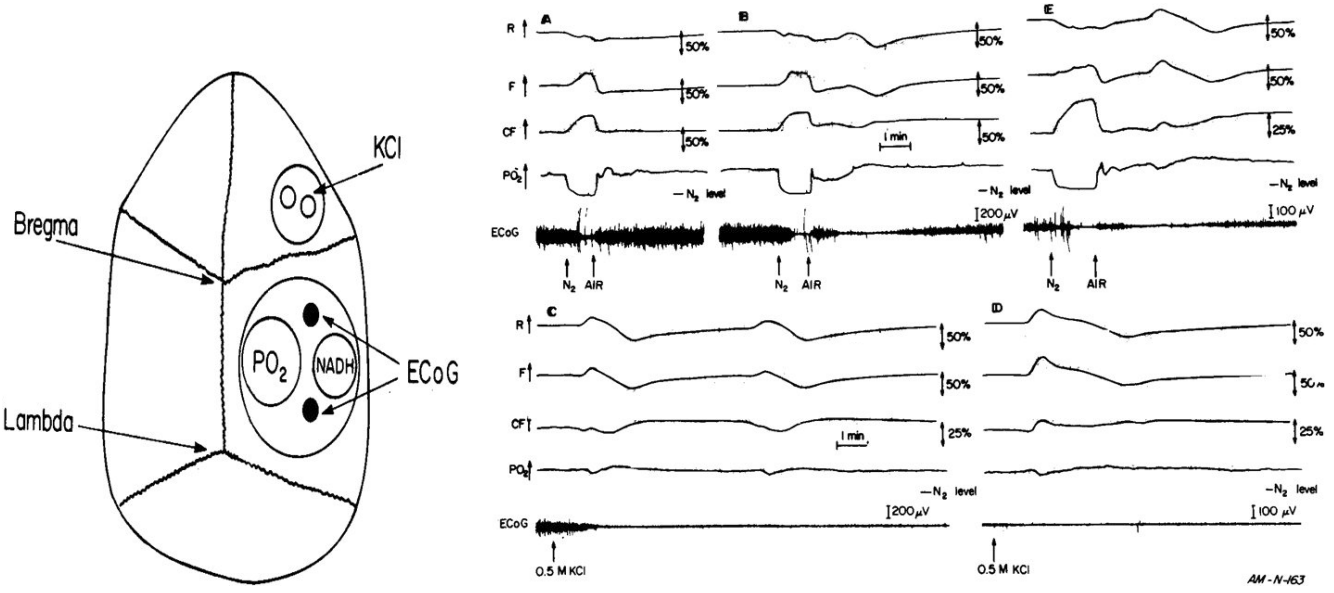

(a) (b)

Fig. 11. (a) A schematic representation of the various probe locations above the brain of the gerbil. The large cannula contains the light guide for NADH measurement, pO_2 and ECoG electrodes. The cannula for KCl application was located 2−3 mm anterior to the large cannula.[20] (b) The effects of anoxia (A, B, E) and spreading depression (C, D) on NADH and pO_2 in the awake (A, B, C) and deeply anesthetized (D, E) gerbil brain.[20]

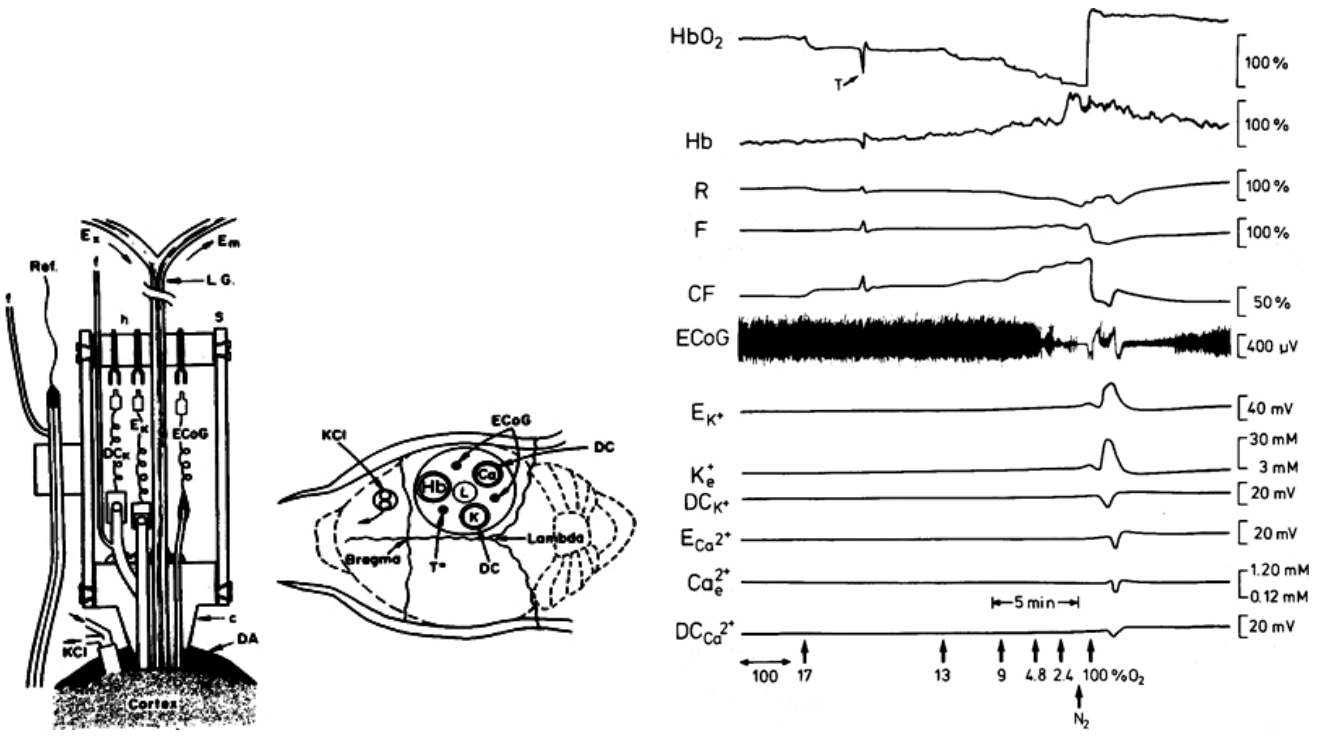

(a) (b)

Fig. 12. (a) The longitudinal section of the MPA (multiprobe assembly, left) and its topical view when located on the gerbil brain.[21] (b) The metabolic, ionic and electrical responses to graded hypoxia induced in the gerbil brain.[3]

microcirculatory blood flow, in addition to NADH, Reflectance, extracellular K^+ and Ca^{2+} and ECoG and DC potential. The *in vivo* multiparametric monitoring approach has also been applied to other organs in the body.

2.3.1. *Multiparametric monitoring Type A*

The first stage that Prof. Chance supported was the addition oxygen electrode to the NADH and EEG monitored. Male gerbils (60−70 g) were used in our study. The animals were anesthetized by intraperitoneal injection of Equithesin (a mixture of pentobarbital, chloral hydrate and magnesium sulfate) 0.3 ml/100 gm. The skull was exposed by a midline incision and a 5- to 6-mm diameter hole was drilled in the parietal bone to fit a combined NADH-pO_2 cannula (Fig. 11, left). A 2-mm diameter hole was drilled in the frontal bone to fit a push-pull cannula for epidural application of KCl in order to elicit cortical SD. Two stainless steel screws were implanted on the left parietal bone for holding the cement to the skull. The cannulae and the screws were cemented to the skull by dental acrylic cement. The oxidation−reduction state of NADH was monitored using a standard DC fluorometer/reflectometer with a 1.5-mm diameter, Y-shaped light guide. The pO_2 was measured by an open-type oxygen electrode, 2.5 mm in diameter. ECoG was measured by two stainless steel rods (0.5 mm in diameter) inserted through the wall of the combined cannula.

The normoxic pO_2 level varied between animals due to the different location in relation to the blood vessels. Figure 11 shows the effects of anoxia and SD on the awake and anesthetized brain.[20] Parts A and B show the responses to two nitrogen cycles. The reflectance and fluorescence responses are typical and NADH became fully reduced within less than 1 min. The decrease in pO_2 had faster kinetics and stayed at the zero level until re-breathing started. The main difference between the two cycles can be seen in the recovery phase from anoxia. In the first cycle (A), the overshoot of the pO_2 was higher than the normoxic level and showed a lower level followed by a small overshoot. At the same time, the NADH showed an oxidation cycle typical for the SD response. The ECoG trace showed a typical anoxic depression in parts A and B and a secondary depression in part B concomitant with the metabolic and hemodynamic responses. In Fig. 11(c), two responses to SD are shown after its elicitation by topical application of KCl solution. The reflectance trace (B) shows a typical biphasic response and the corrected fluorescence (CF) demonstrates the oxidation−reduction cycle. The pO_2 trace presents a decreased level of oxygen during the SD cycles. The ECoG was depressed during the cycles, although the recovery to the original amplitude was very slow (not shown in Fig. 11). Parts D and E show the responses to anoxia and SD in the same gerbil under anesthesia. The pO_2 response to SD in the anesthetized state (part D) is similar to that of the awake brain (part C). On the other hand, the NADH corrected trace shows a reduction cycle rather than the typical oxidation cycle. The response to anoxia in the anesthetized state is shown in part E and is followed by a spontaneous SD cycle as shown in the ECoG trace. The pO_2 trace shows the typical decrease cycle during the SD, concomitant with a reduction cycle of the NADH. The recovery phase from anoxia, as depicted in Figs. 11(A), 11(B) and 11(E), had a special pattern depending on the state of the brain. In part B, the pO_2 trace showed a sharp dip after the fast recovery to the normoxic level, but at the same time, the NADH was also above the normoxic level, so we can conclude that it is not an artifact of the pO_2 electrode. This dip in the pO_2 is not clear in Figs. 11(A) and 11(E), as the NADH trace also recovers to the normoxic level.

2.3.2. *The multiparametric monitoring Type B*

The newly developed Multiparametric Monitoring Assembly (MPA, Fig. 12(a)) provides a simultaneous readout of the tissue energy state, ionic and electrical activities.[3] Tissue oxygen delivery was monitored by the oxy-deoxyhemoglobin ratio, and intracellular O_2 balance was evaluated by the intramitochondrial NADH redox state. This method was introduced to the JF by Prof. Kessler from Germany. He came with his EMPHO device that monitors hemoglobin saturation and spent few weeks with us. The ionic homeostasis was evaluated by monitoring the extracellular K^+ and Ca^{2+} activities reflecting the permeability changes of cation channels as well as the activities of Na^+−K^+− ATPase and other ion-linked transport processes. The electrical activities were monitored by a bipolar electro-cortical surface electrode (ECoG) and changes in the DC steady potential.

Figure 12(b) shows a typical response to graded hypoxia, covering the range from 100% to 0% oxygen in the breathing mixture and then a recovery to 100% O_2 for another 5 min. As observed, a gradual decrease in hemoglobin saturation (HbO_2) was recorded simultaneously with the increase in the intramitochondrial redox state (CF). In parallel, changes were recorded in the reflected light intensity (R) and the Hb concentration, representing the autoregulation response due to the hypoxia. The first change in the ECoG was noted at FiO_2 level below 9% and was severely depressed at 4.8% and became isoelectric under N_2 breathing. The resting level of extracellular K^+ was 2.5 mM and it increased gradually to a maximum of 3.9 mM during the short complete anoxic period. The resting level of Ca^{2+} was quite low as compared to other brains monitored (due to a film of blood below the electrode) and was decreased from 0.6 mM (normoxia) to 0.5 mM during the anoxia. The DC steady potential around the K^+ and Ca^{2+} electrodes showed a 1−2 mV positive change during the hypoxia, but we suspect it was because of a small instability of the reference electrode since it did not recover during the normoxic recovery period.

The recovery period presents a short period of reoxygenation followed by a wave of SD developed probably by the increased K^+ level during the anoxic period. As seen, the brain became hyperoxygenated due to the vasodilated state (at the end of the anoxia) and the breathing of 100% oxygen. The SD episode occurred immediately after the reoxygenation of the brain, showing the typical ionic homeostasis disturbances, namely an increase in extracellular K^+(26.3 mM) and a decrease in Ca^{2+} (0.22 mM). During the recovery from the SD wave, the K^+ showed an undershoot due to the activated Na^+-K^+-ATPase or the higher permeability of K^+ through the plasma membrane. The NADH became more oxidized during the SD cycle, while the blood HbO_2 showed a very small, if at all, transient deoxygenation. The transient change in blood oxygenation and NADH redox state seen during the first step of the hypoxia is due to a short bilateral carotid artery occlusion. This procedure enabled us to determine indirectly the O_2 uptake rate and will be discussed separately.

2.4. *Monitoring inside the ^{31}P NMR magnet*

The pioneering work of Chance and his team in the development of ^{31}P-MRS enabled me to expand my collaborative studies in Philadelphia during 1988−1990. We developed a new multiprobe assembly that can be used inside the magnet, enabling the monitoring of hemodynamic, metabolic, electrical and ionic activities continuously and simultaneously with ^{31}P-MRS. Relative cerebral blood flow (CBF) was measured by a Laser Doppler flowmeter using a fiber optic probe.[38] Mitochondrial activity was evaluated by monitoring the NADH redox state using surface fluorometry.[17,39,40] Ionic homeostasis was evaluated by the extracellular levels of K^+ and Ca^{2+} measured by surface ion-selective mini-electrodes.[41,42] The electrical activities were assessed by the DC steady potential as well as by the ECoG. This study was carried out in order to determine whether it is possible to measure, simultaneously and in real time, parameters that are measurable by the multiprobe assembly together with parameters that are measurable using NMR spectroscopy, so as to more precisely determine injury during pathological conditions or interventions (Fig. 13).[27]

In order to compare the data accumulated by the MPA and the MRS, quantitative analysis of all measured parameters was performed at 5 min intervals. Figure 14 shows typical effects of a 20-min bilateral carotid artery occlusion on the various calculated parameters.[27] Part A exhibits the hemodynamic changes occurring in the three major parameters: CBF, CBV (volume) and NADH redox state. After four control points (total 15 min) ischemia was induced, and CBF and CBV decreased to the minimal levels within 5 min. Concomitantly, the intramitochondrial NADH redox state reached maximal levels. The low CBF and high NADH remained unchanged until the reopening of the two carotid arteries. NADH returned to its pre-ischemic levels within 10 min, while CBF showed a large hyperemic response during the recovery phase. The CBV showed a small overshoot response. The energy state of the gerbil brain during the ischemia is shown in Fig. 14(b). PCr and ATP levels decreased gradually during the ischemic episode and reached minimal levels 15 min after the occlusion. Ten minutes elapsed following the reopening of the vessels, before the high-energy compounds returned to their pre-ischemic levels. The typical disturbances in ionic homeostasis caused by the ischemic event are shown in Fig. 14(c). The major changes in extracellular K^+ and Ca^{2+} occurred during the first 10 min of ischemia followed by small changes during the

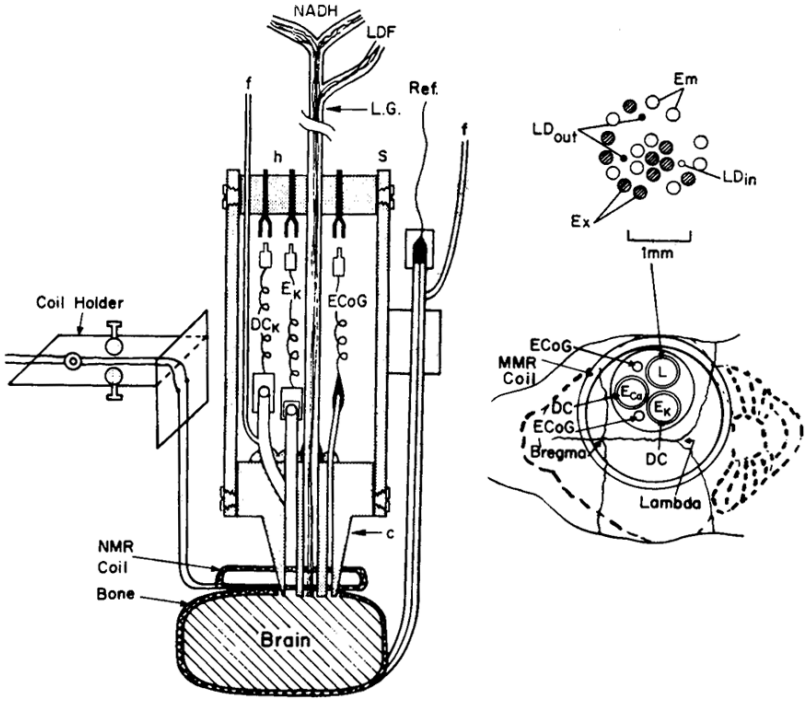

Fig. 13. The experimental setup used in order to monitor brain functions inside the NMR magnet. A longitudinal section of the multiprobe assembly connected to the NMR coil and the gerbil brain is shown on the left. The relative locations of the various probes on the brain are shown on the right. E_K, E^{2+}_{Ca} DC_K, potassium, calcium and DC electrodes; c, plexiglass multiprobe holder; h, connection holder; s, plexiglass sleeve; Ref, reference electrode; F, feeling tube of DC or reference electrode; LG, light guide; Ex, Em, excitation and emission fibers for NADH monitoring; LD_{in} LD_{out}, fibers for CBF monitoring by the Laser Doppler flowmeter.[27]

remaining 10 min. In this specific gerbil, the recovery of the two ions did not exhibit identical kinetics. Most of the K^+ recovered within 10 min (after a slow initial phase), while the recovery of Ca^{2+} was much slower and was complete only after 30 min. The DC steady potential demonstrated a negative shift when measured concentric to the K^+ and Ca^{2+} electrodes. A return of the DC potential to baseline levels occurred after 5−10 min of reperfusion, whereas during the initial 5 min changes were minimal.

2.5. *Monitoring the brain in neurosurgical patients*

As mentioned before, Prof. Chance was able to contribute significant information regarding the human brain in neurosurgical patients. During my two-year visit in the JF (1988−1990) Prof. Chance helped me to start our monitoring of patient. The monitoring of neurosurgical patients started at the University of Pennsylvania.[28] Figure 15 shows the response of the human cerebral cortex to a short ischemic episode induced by occlusion of the carotid artery prepared for the aneurysm procedure.[28] Immediately after the occlusion, a drop in CBF was recorded (a decrease in LDF signal) simultaneously with an increase in NADH redox state (CF signal). Very small changes in the reflected light (R) were recorded during the occlusion. The recovery of the blood flow and the oxidation of NADH were very quick, as seen in both traces. A large overshoot in CBF was noted without a parallel undershoot in the NADH redox state during the reperfusion period, as was also found in animal models exposed to ischemic conditions.

3. Discussion

This paper summarizes four decades of our collaboration with Prof. Britton Chance in studying mitochondrial function *in vivo* under various pathophysiological conditions. In blood perfused organs, the use of optical techniques is subject to various artifacts such as changes in blood volume or hemoglobin oxygenation. In our experience, the monitoring of various components of the respiratory chain is prone to those artifacts. We found that the NADH redox state, measured by fluorometry, is the

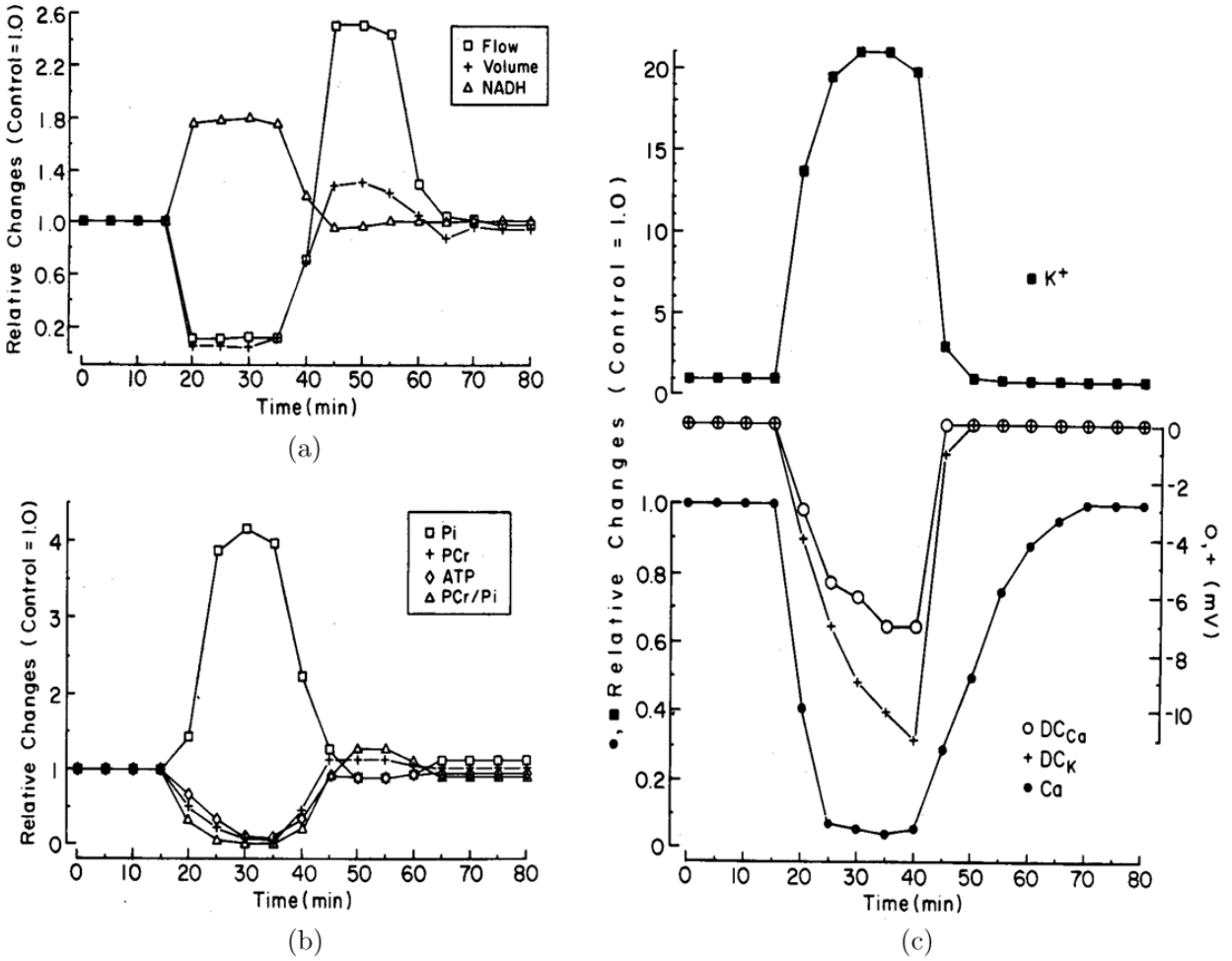

Fig. 14. Typical changes of the various parameters monitored from the gerbil brain located in the NMR magnet and exposed to 20 min ischemia. The original numbers measured were normalized in order to present a few of them on the same ordinate scale. Only the DC potential is presented in absolute units (mv). (a) Cerebral blood flow and volume, NADH redox state; (b) Pi, PCr, ATP PCr/Pi; (c) Extracellular levels of K^+ and Ca^{2+}, DC^{2+}_{Ca}, DC^{+}_{K}, steady potentials around the ion selective electrodes.[27]

best and most practical parameter to evaluate mitochondrial function and tissue oxygen balance in real time. Tissue vitality is correlated with oxygen or energy balance defined as the ratio between oxygen supply and demand. Energy or oxygen supply mechanisms are identical in all tissues and therefore could be monitored by the same monitoring technique in various body organs.

Nevertheless, due to the complexity of biological systems, monitoring a single parameter such as NADH redox state is insufficient. The limitation is that this parameter, when monitored alone, represents both the intracellular oxygen level and the balance between oxygen demand and supply. Therefore, the addition of other parameters, such as tissue blood flow and hemoglobin oxygenation, is highly desirable. The O_2 supply is affected by the dynamic changes in the microcirculatory blood flow and by the level of HbO_2. The higher the flow and hemoglobin oxygenation, the better is the oxygen supply.

In addition to the in-depth survey of NADH measurement in experimental animals, the present work suggests the potential use of NADH monitoring in a medical device. This new device enables the monitoring of microcirculatory hemoglobin oxygenation together with the parameters of tissue microcirculatory blood flow, reflectance and mitochondrial NADH redox state.[43] As the present results show, mitochondrial NADH is the most stable and representative parameter of tissue energy metabolism in the intracellular space. It is affected by substrate and O_2 availability and ATP turnover, determined by the metabolic activity of the tissue.

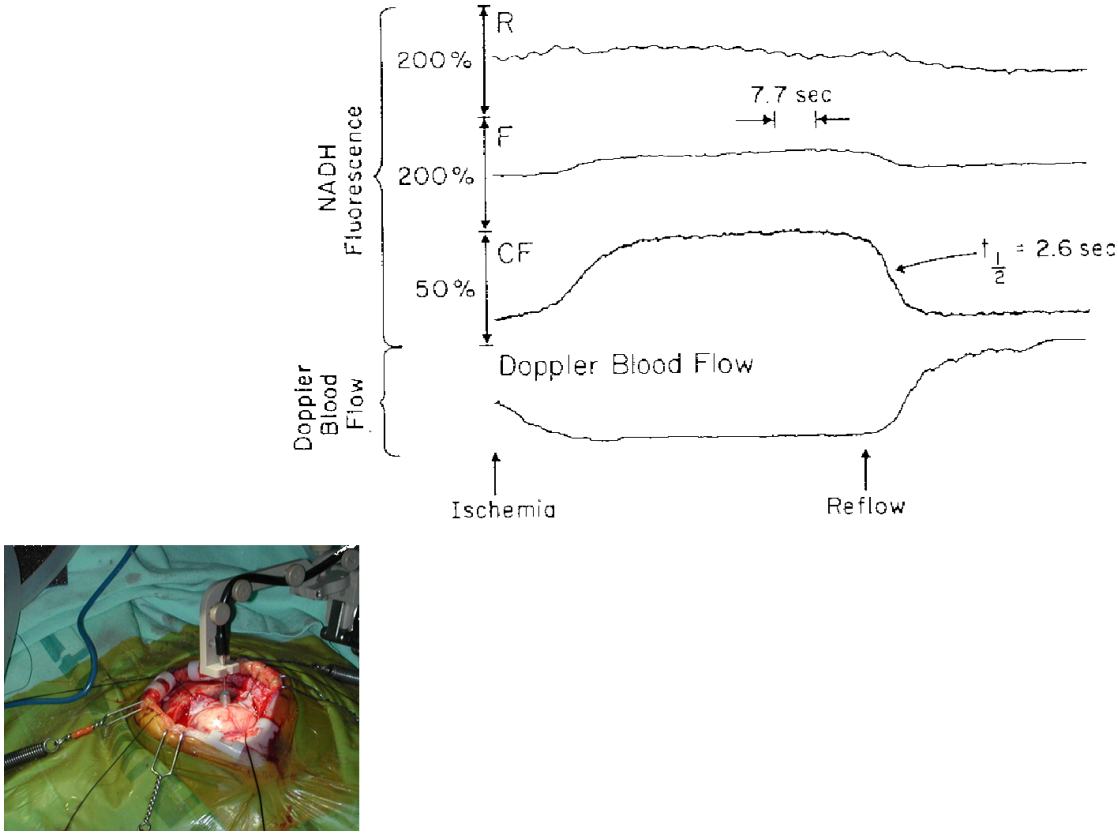

Fig. 15. The response of the human brain to a short episode of ischemia induced by ligation of the carotid artery during a neurosurgical procedure. The small picture presents a possible probe that could be located on the brain in the operating room.[28]

The inter-related CBF and HbO_2 are more sensitive to instability in the regulation of blood flow, which is influenced by many factors (NO, CO_2, pH) and not only by oxygen consumption.

The significance of multiparametric tissue monitoring is demonstrated by the present typical results of concomitant TBF and NADH redox measurements (Fig. 12). Here, the control levels of the normoxic tissue are defined as 100% and changes are expressed by an increase or decrease relative to the control values. The results accumulated in preliminary clinical studies (Fig. 15) suggest that the monitoring of the patients' brain or other organs is practical and can provide critical information for patient care.

References

1. A. Mayevsky, B. Chance, "A new long-term method for the measurement of NADH fluorescence in intact rat brain with implanted cannula," *Int. Symp. Oxygen Transport to Tissue, Adv. Exp. Med. Biol.*, pp. 239–244, Plenum Press, New York (1973).
2. B. Chance, N. Oshino, T. Sugano, A. Mayevsky, "Basic principles of tissue oxygen determination from mitochondrial signals," *Oxygen Transport to Tissue. Instrumentation, Methods, and Physiology*, H. I. Bicher, D. F. Bruley, Eds., pp. 277–292, Plenum Publishing Corporation, New York (1973).
3. A. Mayevsky, D. Jamieson, B. Chance, "Oxygen poisoning in unanesthetized brain: Correlation of pyridine nucleotide redox state and electrical activity," *Brain Res.* **76**, 481–491 (1974).
4. A. Mayevsky, B. Chance, "Repetitive patterns of metabolic changes during cortical spreading depression of the awake rat," *Brain Res.* **65**, 529–533 (1974).
5. A. Mayevsky, B. Chance, "Metabolic responses of the awake cerebral cortex to anoxia hypoxia spreading depression and epileptiform activity," *Brain Res.* **98**, 149–165 (1975).
6. A. Mayevsky, B. Chance, "The effect of decapitation on the oxidation–reduction state of NADH and ECoG in the brain of the awake rat," *Oxygen Transport to Tissue II, Adv. Exp. Med. Biol.*, pp. 307–312, Plenum Press, New York (1976).
7. B. Chance, A. Mayevsky, C. Goodwin, L. Mela, "Factors in oxygen delivery to tissue," *Microvasc. Res.* **8**, 276–282 (1974).

8. M. Osbakken, A. Mayevsky, I. Ponomarenko, D. Zhang, C. Duska, B. Chance, "Combined *in vivo* NADH fluorescence and ^{31}P-NMR to evaluate myocardial oxidative phosphorylation," *J. Appl. Cardiol.* **4**, 305−313 (1989).
9. M. Osbakken, M. Mitchell, D. Zhang, A. Mayevsky, B. Chance, "*In vivo* correlation of myocardial metabolism, perfusion and mechanical function during increased cardiac work," *Cardiovasc. Res.* **25**, 749−756 (1991).
10. B. R. Silberstein, A. Mayevsky, B. Chance, "Metabolic responses of the gerbil brain cortex to anoxia, spreading depression, carotid occlusion and stroke," *Frontiers in Bioenergetics*: *From Electrons to Tissues*, P. L. Dutton, J. Leigh, A. Scarpa, Eds., pp. 1477−1485, Academic Press, New York (1978).
11. B. Chance, C. Barlow, Y. Nakase, H. Takeda, A. Mayevsky, R. Fischetti, N. Graham, J. Sorge, "Heterogeneity of oxygen delivery in normoxic and hypoxic states: A fluorometer study," *Am. J. Physiol.* **235**, H809−H820 (1978).
12. B. Chance, C. Barlow, J. Haselgrove, Y. Nakase, B. Quistorff, F. Matschinsky, A. Mayevsky, "Microheterogeneities of redox states of perfused and intact organs," in *Microenvironments and Metabolic Compartmentation*, P. Srere, Ed., pp. 221−232, Academic Press, New York (1978).
13. B. Chance, B. R. Silberstein, A. Mayevsky, "Heterogeneity of metabolic states of the cerebral cortex *in vivo*," *Cerebral Metabolism and Neural Function*, J. V. Passoneau, R. A. Hawkins, W. D. Lust, F. A. Welsh, Eds., pp. 77−84, Williams & Wilkins, Baltimore/London (1980).
14. B. R. Silberstein, A. Mayevsky, B. Chance, "Flying spot studies of brain flavoproteins in the gerbil," *Neurol. Res.* **2**, 19−34 (1980).
15. A. Mayevsky, H. Kaplan, J. Haveri, J. Haselgrove, B. Chance, "Three-dimensional metabolic mapping of the freeze-trapped brain: Effects of ischemia on the Mongolian gerbil," *Brain Res.* **367**, 63−72 (1986).
16. J. C. Haselgrove, C. L. Bashford, C. H. Barlow, B. Quistorff, B. Chance, A. Mayevsky, "Time resolved 3-D recording of redox ratio during spreading depression in gerbil brain," *Brain Res.* **506**, 109−114 (1990).
17. A. Mayevsky, B. Chance, "Intracellular oxidation reduction state measured *in situ* by a multichannel fiber-optic-surface fluorometer," *Science* **217**, 537−540 (1982).
18. A. Mayevsky, B. Chance, "Multisite measurements of NADH redox state from cerebral cortex of the awake animal," *Oxygen Transport to Tissue, IV*, H. I. Bicher and D. F. Bruley, Eds., pp. 143−155, Plenum Publishing Corporation, New York (1983).
19. A. Mayevsky, T. Zeuthen, B. Chance, "Measurements of extracellular potassium, ECoG and pyridine nucleotide levels during cortical spreading depression in rats," *Brain Res.* **76**, 347−349 (1974).
20. A. Mayevsky, S. Lebourdais, B. Chance, "The interrelation between brain PO_2 and NADH oxidation−reduction state in the gerbil," *J. Neurosci. Res.* **5**, 173−182 (1980).
21. A. Mayevsky, K. H. Frank, S. Nioka, M. Kessler, B. Chance, "Oxygen supply and brain function *in vivo*: A multiparametric monitoring approach in the Mongolian gerbil," *Oxygen Transport to Tissue XII*, J. Piiper, T. K. Goldstick, M. Meyer, Eds., pp. 303−313, Plenum Press, New York (1990).
22. A. Mayevsky, K. Frank, M. Muck, S. Nioka, M. Kessler, B. Chance, "Multiparametric evaluation of brain functions in the Mongolian gerbil *in vivo*," *J. Basic Clin. Physiol. Pharmacol.* **3**, 323−342 (1992).
23. A. Mayevsky, V. H. Subramanian, S. Nioka, C. Barlow, J. Haselgrove, B. Chance, "Brain energy metabolism evaluated simultaneously in the newborn dog by ^{31}P-NMR spectroscopy and NADH fluorometry/reflectometry *in vivo*," *J. CBF Metab.* Suppl., pp. 400−401 (1985).
24. A. Mayevsky, S. Nioka, V. H. Subramanian, B. Chance, "Microcirculatory responses to brain hypoxia in the newborn dog as evaluated by P-NMR spectroscopy and NADH fluorometry/reflectometry *in vivo*," *Microcirculation — An Upadate*, M. Tsuchiya, M. Asano, Y. Mishima, M. Oda, Eds., pp. 49−50, Excerpta Medica, Amsterdam (1987).
25. A. Mayevsky, S. Nioka, B. Chance, "Fiber optic surface fluorometry/reflectometry and ^{31}P-NMR for monitoring the intracellular energy state *in vivo*," *Oxygen Transport to Tissue X*, M. Mochizuki, C. R. Honig, T. Koyama, T. K. Goldstick, D. F. Bruley, Eds., pp. 365−374, Plenum Press, New York (1988).
26. A. Mayevsky, S. Nioka, V. H. Subramanian, B. Chance, "Brain oxidative metabolism of the newborn dog: Correlation between ^{31}P-NMR spectroscopy and pyridine nucleotides redox state," *J. CBF Metab.* **8**, 201−207 (1988).
27. A. Mayevsky, S. Nioka, D. J. Wang, B. Chance, "The functioning gerbil brain *in vivo*: Correlation between ^{31}P-NMR spectroscopy and the multiparametric monitoring approach," *Oxygen Transport to Tissue XVIII*, E. M. Nemoto, J. C. LaManna, Eds., pp. 41−53, Plenum Press, New York (1997).
28. A. Mayevsky, E. S. Flamm, W. Pennie, B. Chance, "A fiber-optic-based multiprobe system for intraoperative monitoring of brain functions," *SPIE Proc.* **1431**, 303−313 (1991).

29. A. Mayevsky, B. Chance, "Oxidation−reduction states of NADH *in vivo*: From animals to clinical use," *Mitochondrion* **7**, 330−339 (2007).
30. M. Maris, A. Mayevsky, B. Chance, "Frequency domain dynamic measurements of changes of optical pathlength during spreading depression in rodent brain mode," *SPIE Proc.* **1431**, 136−148 (1991).
31. B. Chance, A. Mayevsky, B. Guan, Y. Zhang, "Hypoxia/ischemia triggers a light scattering event in rat brain," *Adv. Exp. Med. Biol.* **428**, 457−467 (1997).
32. S. Nioka, B. Chance, D. S. Smith, A. Mayevsky, M. P. Reilly, C. Alter, T. Asakura, "Cerebral energy metabolism and oxygen state during hypoxia in neonate and adult dogs," *Pediatr. Res.* **28**, 54−62 (1990).
33. S. Nioka, D. S. Smith, A. Mayevsky, G. Dobson, R. L. Veech, H. Subramanian, B. Chance, "Age dependence of steady state mitochondrial oxidative metabolism in the *in vivo* g hypoxic dog brain," *Neurol. Res.* **13**, 25−32 (1991).
34. A. Mayevsky, G. G. Rogatsky, "Mitochondrial function *in vivo* evaluated by NADH fluorescence: From animal models to human studies," *Am. J. Physiol. Cell. Physiol.* **292**, C615−C640 (2007).
35. A. Mayevsky, "Brain energy metabolism of the conscious rat exposed to various physiological and pathological situations," *Brain Res.* **113**, 327−338 (1976).
36. B. Chance, V. Legallias, B. Schoener, "Combined fluorometer and double-beam spectrophotometer for reflectance measurements," *Rev. Sci. Instrum.* **34**, 1307−1311 (1963).
37. F. F. Jöbsis, W. N. Stainsby, "Oxidation of NADH during contractions of circulated mammalian skeletal muscle," *Respir. Physiol.* **4**, 292−300 (1968).
38. A. Mayevsky, C. M. Friedli, M. Reivich, "Metabolic, ionic and electrical responses of the gerbil brain to ischemia," *Am. J. Physiol.* **248**, R99−R107 (1985).
39. A. Mayevsky, U. Marchaim, "Studies on the effect of Iucerne saponines on the respiration of cottonseeds using $^{18}O_2$," *Plant Cell Physiol.* **13**, 927−930 (1972).
40. A. Mayevsky, D. Samuel, S. S. Friedland, J. H. Ewins, "*In vivo* measurement of ^{32}P in the brain of a freely moving rat," *J. Neurosci. Res.* **1**, 275−286 (1975).
41. J. Sonn, A. Mayevsky, "The effect of ethanol on metabolic, hemodynamic and electrical responses to cortical spreading depression," *Brain Res.* **908**, 174−186 (2001).
42. K. C. Wadhwani, S. I. Rapoport, "Blood flow in the central and peripheral nervous systems," *Laser Doppler Blood Flowmetry*, A. P. Shephard and P. A. Oberg, Eds., pp. 265−304, Kluwer Academic Pub., Boston (1990).
43. B. Chance, P. Cohen, F. Jöbsis, B. Schoener, "Intracellular oxidation−reduction states *in vivo*," *Science* **137**, 499−508 (1962).
44. A. Mayevsky, "Brain NADH redox state monitored *in vivo* by fiber optic surface fluorometry," *Brain Res. Rev.* **7**, 49−68 (1984).
45. W. Crowe, A. Mayevsky, L. Mela, "Application of a solid membrane ion selective electrode to *in vivo* measurements," *Am. J. Physiol.* **233**, C56−C60 (1977).
46. E. Yoles, N. Zarchin, A. Mayevsky, "Effects of age on the metabolic ionic and electrical responses to anoxia in the newborn dog brain *in vivo*," *J. Basic Clin. Physiol. Pharmacol.* **2**, 297−313 (1991).
47. A. Mayevsky, Y. Blum, N. Dekel, A. Deutsch, R. Halfon, S. Kremer, E. Pewzner, E. Sherman, O. Barnea, "The CritiView — A new fiber-optic-based optical device for the assessment of tissue vitality," *Proc. SPIE* **6083**, 60830Z-1−60830Z-9 (2006).
48. A. Harden, W. Young, "The alcoholic ferment of yeast-juice," *Proc. Roy. Soc.* **77**, 405−120 (1906).
49. O. Warburg, W. Christian, A. Griese, "Hydrogen transferring coenzyme; its composition and mode of action," *J. Biochem.* **282**, 157−205 (1935).
50. O. Warburg, W. Christian, *Biochem. Z* **287**, 291 (1936).
51. H. Theorell, R. Bonnichsen, "Studies on liver alcohol dehydrogenase. I. Equilibria and initial reaction velocities," *Acta Chem. Scand.* **5**, 1105−1126 (1951).
52. B. Chance, V. Legallias, "Rapid and sensitive spectrophotometry. A stopped-flow attachment for a stabilized quartz spectrophotometer," *Rev. Sci. Instrum.* **22**, 627−638 (1951).
53. B. Chance, J. B. Neilands, "Studies on lactic dehydrogenase of heart. II. A compound of lactic dehydrogenase and reduced pyridine nucleotide," *J. Biol. Chem.* **199**, 383−387 (1952).
54. B. Chance, "Spectrophotometry of intracellular respiratory pigments," *Science* **120**, 767−775 (1954).
55. B. Chance, G. R. Williams, "Respiratory enzymes in oxidative phosphorylation. III. The steady state," *J. Biol. Chem.* **217**, 409−427 (1955).
56. L. N. M. Duysens, J. Amesz, "Fluorescence spectrophotometry of reduced phosphopyridine nucleotide in intact cells in the near-ultraviolet and visible region," *Biochim. Biophys. Acta* **24**, 19−26 (1957).
57. B. Chance, H. Baltscheffsky, "Respiratory enzymes in oxidative phosphorylation," *J. Biol. Chem.* **233**, 736−739 (1958).
58. B. Chance, F. Jöbsis, "Changes in fluorescence in a frog sartorius muscle following a twitch," *Nature* **184**, 195−196 (1959).

59. B. Chance, V. Legallias, B. Schoener, "Metabolically-linked changes in fluorescence emission spectra of cortex of rat brain, kidney and adrenal gland," *Nature* **195**, 1073−1075 (1962).
60. B. Chance, D. Jamieson, H. Coles, "Energy-linked pyridine nucleotide reduction: Inhibitory effects of hyperbaric oxygen *in vitro* and *in vivo*," *Nature* **206**, 257−263 (1965).
61. F. F. Jöbsis, M. O'Connor, A. Vitale, H. Vreman, "Intracellular redox changes in functioning cerebral cortex. I. Metabolic effects of epileptiform activity," *Neurophysiology* **34**, 735−749 (1971).
62. F. F. Jöbsis, M. J. O'Conner, M. Rosenthal, J. M. VanBuren, "Fluorometric monitoring of metabolic activity in the intact cerebral cortex," in *Neurophysiology Studied in Man*, pp. 18−26, Excerpta Medica, Amsterdam (1971).
63. A. Mayevsky, A. Doron, T. Manor, S. Meilin, N. Zarchin, G. E. Ouaknine, "Cortical spreading depression recorded from the human brain using a multiparametric monitoring system," *Brain Res.* **740**, 268−274 (1996).
64. A. Mayevsky, T. Manor, E. Pewzner, A. Deutsch, R. Etziony, N. Dekel, "Real time optical monitoring of tissue vitality *in vivo*," *SPIE* **4616**, 30−39 (2002).